11-9-2016

Mesenteric Vascular Dysregulation and Intestinal Inflammation Accompanies Experimental Spinal Cord Injury

Emily Swartz Besecker
Gettysburg College

Gina M. Deiter
Penn State College of Medicine

Nicole Pironi
Muhlenberg College

Timothy K. Cooper
The Pennsylvania State University College of Medicine

Gregory Michael Holmes
Penn State College of Medicine

Recommended Citation

Besecker, Emily Swartz, Gina M. Deiter, Nicole Pironi, Timothy K. Cooper, and Gregory Michael Holmes. "Mesenteric Vascular Dysregulation and Intestinal Inflammation Accompanies Experimental Spinal Cord Injury." American Journal of Physiology-Regulatory, Integrative and Comparative Physiology (2016).

Mesenteric Vascular Dysregulation and Intestinal Inflammation Accompanies Experimental Spinal Cord Injury

Abstract

Cervical and high thoracic spinal cord injury (SCI) drastically impairs autonomic nervous system function. Individuals with SCI at thoracic spinal-level 5 (T5) or higher often present cardiovascular disorders that include resting systemic arterial hypotension. Gastrointestinal (GI) tissues are critically dependent upon adequate blood flow and even brief periods of visceral hypoxia triggers GI dysmotility. The aim of this study was to test the hypothesis that T3-SCI induces visceral hypoperfusion, diminished postprandial vascular reflexes and concomitant visceral inflammation. We measured in vivo systemic arterial blood pressure and superior mesenteric artery (SMA) and duodenal blood flow in anesthetized T3-SCI rats at 3 days and 3 weeks post-injury either fasted or following enteral feeding of a liquid mixed-nutrient meal (Ensure™). In separate cohorts of fasted T3-SCI rats, markers of intestinal inflammation were assayed by qRT-PCR. Our results show that T3-SCI rats displayed significantly reduced SMA blood flow under all experimental conditions ($p<0.05$). Specifically, the anticipated elevation of SMA blood flow in response to duodenal nutrient infusion (postprandial hyperemia) was either delayed or absent after T3-SCI. The dysregulated SMA blood flow in acutely-injured T3-SCI rats coincides with abnormal intestinal morphology and elevation of inflammatory markers, all of which resolve after 3 weeks. Specifically, Icam1, Ccl2 (MCP-1) and Ccl3 (MIP-1α) were acutely elevated following T3-SCI. Our data suggest that arterial hypotension diminishes mesenteric blood flow necessary to meet mucosal demands at rest and during digestion. The resulting GI ischemia and low-grade inflammation may be an underlying pathology leading to GI dysfunction seen following acute T3-SCI.

Keywords

spinal cord injury, in vivo studies, inflammation, gastrointestinal dysmotility, ileus

Disciplines

Anatomy | Medicine and Health Sciences

Articles in PresS. Am J Physiol Regul Integr Comp Physiol (November 9, 2016). doi:10.1152/ajpregu.00347.2016

Mesenteric vascular dysregulation and intestinal inflammation accompanies experimental spinal cord injury

Emily M. Besecker[1], Gina M. Deiter[2], Nicole Pironi[3], Timothy K. Cooper[4], Gregory M. Holmes[1*]

[1] Department of Neural & Behavioral Sciences, Penn State University College of Medicine, USA

[2] Department of Cellular and Molecular Physiology, Penn State University College of Medicine, USA

[3] Department of Biology, Muhlenberg College, USA

[4] Department of Comparative Medicine, Penn State University College of Medicine, USA

Corresponding author:

Gregory M. Holmes

Department of Neural & Behavioral Sciences, Penn State University College of Medicine,

500 University Drive

Hershey, PA 17033

Email: gmh16@psu.edu

Running title: Mesenteric hypoperfusion in SCI

ABSTRACT

Cervical and high thoracic spinal cord injury (SCI) drastically impairs autonomic nervous system function. Individuals with SCI at thoracic spinal level 5 (T5) or higher often present cardiovascular disorders that include resting systemic arterial hypotension. Gastrointestinal (GI) tissues are critically dependent upon adequate blood flow and even brief periods of visceral hypoxia triggers GI dysmotility. The aim of this study was to test the hypothesis that T3-SCI induces visceral hypoperfusion, diminished postprandial vascular reflexes and concomitant visceral inflammation. We measured *in vivo* systemic arterial blood pressure and superior mesenteric artery (SMA) and duodenal blood flow in anesthetized T3-SCI rats at 3 days and 3 weeks post-injury either fasted or following enteral feeding of a liquid mixed-nutrient meal (Ensure™). In separate cohorts of fasted T3-SCI rats, markers of intestinal inflammation were assayed by qRT-PCR. Our results show that T3-SCI rats displayed significantly reduced SMA blood flow under all experimental conditions ($p<0.05$). Specifically, the anticipated elevation of SMA blood flow in response to duodenal nutrient infusion (postprandial hyperemia) was either delayed or absent after T3-SCI. The dysregulated SMA blood flow in acutely-injured T3-SCI rats coincides with abnormal intestinal morphology and elevation of inflammatory markers, all of which resolve after 3 weeks. Specifically, *Icam1*, *Ccl2* (MCP-1) and *Ccl3* (MIP-1α) were acutely elevated following T3-SCI. Our data suggest that arterial hypotension diminishes mesenteric blood flow necessary to meet mucosal demands at rest and during digestion. The resulting GI ischemia and low-grade inflammation may be an underlying pathology leading to GI dysfunction seen following acute T3-SCI.

Keywords:

spinal cord injury, in vivo studies, inflammation, gastrointestinal dysmotility, ileus

Introduction

In addition to the catastrophic sensory and motor losses following spinal cord injury (SCI), autonomic nervous system dysfunction is also widely recognized (30). Furthermore, gastrointestinal (GI) dysmotility is observed clinically immediately after SCI (28, 71) and may persist for years after the initial injury (3, 12, 14, 37, 53, 56, 70). Dysfunction of the digestive organs following experimental SCI includes reduced gastric motility and gastric emptying, abnormal response to GI peptides and reduced nutrient absorption. Each of these co-morbidities contributes to diminished long-term quality of life after SCI (43).

The principal functions of the GI tract, the digestion and absorption of nutrients and the maintenance of proper fluid balance, require adequate blood flow to GI tissues. The primary vascular perfusion occurs through the splanchnic vascular bed that consists of the celiac, superior mesenteric, and inferior mesenteric arteries (35). The distal esophagus, stomach and the proximal duodenum are vascularized by the celiac trunk which supplies three main branches: the left gastric artery, the common hepatic artery, and the splenic artery. The left and right gastric arteries are responsible for the lesser curvature, while the left gastroepiploic and right gastroepiploic arteries feed the greater curvature. The duodenum has a "dual" blood supply, arising from both the celiac trunk and the superior mesenteric artery (SMA). This vascular arrangement reflects the importance of blood supply, and the GI tract is one of the most highly perfused organ systems in the body whereby resting GI blood flow can reach approximately 20-25% of the total cardiac output (10).

Postprandial hyperemia, the global increase in blood flow to the GI tract following a meal, is a critical reflex for adequate GI function and has been demonstrated to result from the exposure of the intestinal mucosa to nutrients in concert with the release of GI peptides (11). The postprandial reflex involves a concurrent increase in blood flow through both the celiac and

superior mesenteric arteries (58). Multiple mechanisms responsible for postprandial hyperemia have been proposed including local presynaptic activation of vasodilation by nitric oxide release (48), vago-vagal reflex activation (33) and inhibition of medullary presympathetic vasomotor neurons by vagal afferent input (50).

Individuals with spinal cord lesions, particularly those rostral to T5, present with diminished sympathetic tone due to disruption of the descending fibers of the medullary presympathetic vasomotor neurons. Loss of these presympathetic vasomotor neurons provokes cardiovascular instability, arterial hypotension, and pooling of blood in the extremities that has been documented clinically (68) and experimentally (31). Vascular hypotension and pooling of blood in the extremities may predispose the GI tract to hypoperfusion following SCI.

Reduced GI blood flow over an extended period of time deprives GI tissues of the oxygen needed to maintain organ integrity (11). The resulting ischemia and restoration of adequate blood flow provokes a multifactorial tissue injury response including a) intercellular adhesion molecule-1 (*Icam1*) mediated increase in adherent leukocytes; b) upregulation of chemokines, particularly monocyte chemotactic protein (*Ccl2*); c) macrophage activation by macrophage inflammatory protein-1α (*Ccl3*); and d) pro-inflammatory cytokines including tumor necrosis factor-α, interleukin (IL)1β and IL6 (19, 67).

In the present work, we employed our established rodent model of T3 spinal level SCI to investigate 1) if T3-SCI leads to reduced mean arterial blood pressure (BP) and reduced resting blood flow within the superior mesenteric artery supplying the mesenteric bed; 2) if T3-SCI diminishes postprandial vascular reflexes; 3) if local duodenal tissue perfusion increases in response to nutrient infusion; and 4) if T3-SCI provokes concomitant histopathologic changes and inflammation of the small intestine.

Methods

All procedures were performed following National Institutes of Health guidelines and under the approval of the Institutional Animal Care and Use Committee at the Penn State University College of Medicine.

Animals

Male Wistar rats (Hsd:WI, Stock 001, Harlan, Indianapolis, IN, USA) ≥8 weeks of age, initially weighing 175-200 g, were used for all experimental procedures. Rats (n=116) were housed in a temperature-controlled room (23°C) on a 12:12-h light-dark cycle with unlimited access to food and water. Following surgical manipulation, rats were housed singly and observed twice a day. Each rat was randomly assigned to one of two surgical manipulations; surgical controls (in which the T3 spinal cord was exposed by laminectomy) or T3-SCI. At the same time, animals were also randomly assigned to one of two post-surgical survival times.

Surgical Procedures and Animal Care

Animals were anesthetized with a mixture of 3-5% isoflurane in oxygen (400-600ml/min) and surgery for T3-SCI using the Infinite Horizons device was performed using established aseptic surgical techniques. When the rat was no longer responsive to toe pinch or palpebral reflex, the surgical site overlying the vertebrae from the interscapular region to mid-thoracic region was shaved and cleaned with three alternating scrubs of chlorhexidine and alcohol. Animals were maintained at 35.5–37.5°C on a feedback-controlled heating block, and rectal temperature was monitored continuously. The location of the elongated T1 and T2 spinous processes were determined by midline palpation. A 3-5cm midline incision of the skin overlying the T1-T3 vertebrae was performed and the muscle attachments to the T1-T3 vertebrae were

cleared by blunt dissection, taking care not to damage the vascular supply to the dorsal nuchal adipose tissue. Using fine-tipped rongeurs, the spinous process and the laminae of the T2 vertebra were removed laterally to the superior articular processes.

Rats receiving T3-SCI (n=61) were transferred to the Infinite Horizons spinal contusion injury device (Precision Systems and Instrumentation, Fairfax, VA, USA). The adjacent T1 and T3 vertebrae were secured into the device and the torso of the animal was suspended slightly above the platform. After centering the exposed spinal cord beneath the impactor tip, a 300 kDyne impact (15 second dwell time) was initiated. This level of injury produces a consistent and reliable neurological and histological outcome whereby animals exhibit a residual, chronic, locomotor deficit and severe loss of the spinal cord white matter. After removal from the contusion device, all surgical incisions were closed in reverse anatomical order with absorbable suture (Vicryl 4-0) for internal sutures and skin closure with wound clips. Wound clips were removed 5-7 days following surgery. Surgical controls (n=55) underwent all procedures except for the contusion injury. A total of 8 T3-SCI rats were lost from the study. Two rats died from unspecified surgical complications (one destined for 3 day *in vivo* physiology, one destined for 3 week tissue harvest) and six rats (all utilized for 3 day *in vivo* physiology) were removed following *post hoc* verification of inadequate lesion severity.

Post-operatively, rats were administered supplemental fluids by subcutaneous injection of 5cc warmed lactated Ringer's solution and stabilized in an incubator (37ºC) until fully recovered from anesthesia. Afterward, animals were monitored daily for any signs of infection or complications from surgery. Rats received extended-release analgesics (buprenorphine SR, 1mg/kg IP, Pfizer Animal Health, Lititz, PA) at time of surgery then antibiotics (enrofloxacin, 2.5 mg/kg) and subcutaneous supplemental fluids (5-10 cc lactated Ringers) twice daily for five

days after surgery. Due to the reduction in locomotor capacity after T3-SCI, a reservoir of chow was placed at head level in order to facilitate ease of access for feeding. All T3-SCI rats ingested a measureable amount each day, thereby confirming that access to chow was available. Body weights and food weights were recorded each morning. T3-SCI rats received bladder expression and ventrum inspection twice daily until the return of spontaneous voiding occurred.

In vivo physiological instrumentation

After 3-days (n=17 T3-SCI, n=18 control) or 3-weeks (n=5 T3-SCI, n=5 control) following the initial surgery, animals were fasted overnight, water provided *ad libitum*, prior to being deeply re-anesthetized with isoflurane (3-5%, 400-600ml/min flow rate) for *in vivo* physiological instrumentation. Animals were placed on a feedback-controlled warming pad (TCAT 2LV, Physitemp Instruments, Clifton, New Jersey) and maintained at 37±1 °C for the duration of the experiment.

Tracheal cannulation - Once fully anesthetized for physiological instrumentation, the animal was tracheally intubated by way of a 1-2-cm midline incision on the ventral side of the neck caudal to the mandible towards the sternal notch. The underlying strap muscles were separated using blunt dissection at the midline to expose the trachea. The exposed trachea was isolated from the underlying esophagus in order to place a loop of 3-0 ethilon suture between the trachea and esophagus to form a ligature. The trachea was opened ventrally by making a small cut in the membrane between two of the cartilaginous rings of the trachea just inferior to the thyroid gland. A small piece of polyethylene tubing (PE-270, 5mm in length and beveled at one end) was inserted into the trachea and secured in place with the ligature. The strap muscles were returned to their proper anatomical location and the overlying skin was secured around the

tracheal tube with 3-0 ethilon. Tracheal intubation maintains an open airway and facilitates clearing of respiratory secretions if necessary.

Femoral arterial and venous catheterization - Following intubation, the femoral artery and adjacent vein or tributaries were exposed, within the region of the femoral triangle, via a small skin incision at the intersection of the inguinum and proximal thigh. Connective tissue was cleared from the femoral artery and vein proximally to the inguinal ligament. The proximal and distal extremes of the exposed artery were gently ligated with 4-0 silk suture. To monitor arterial blood pressure, the femoral artery was hemisected and a sterile PE-50 catheter was inserted in the direction of the abdominal aorta towards the heart. In order to avoid disrupting the arterial endothelium, thus potentially confounding aterial pressure readings, the femoral catheter pressure was advanced so that it terminated in the larger diameter common iliac or in the descending aorta where chance of disrupting the endothelium is reduced. The proximal end of the artery and catheter were fully secured with the 4-0 silk suture and exteriorized. The wound margin was closed with wound clips.

Transonic flow probe - Animals were simultaneously weaned off isoflurane inhalation and deeply anesthetized with thiobutabarbital (Inactin; Sigma, St. Louis, MO; 75-150 mg/kg i.v.) which does not affect long-term cardiovascular (7) or gastrointestinal (45) autonomic function. The rate of Inactin infusion was monitored in conjunction with a resulting momentary drop in arterial BP that quickly returns to normal (SYS-BP1, World Precision Instruments, Sarasota, FL). Once a deep state of anesthesia was achieved, a midline laparotomy was made and the intestines were gently displaced laterally to allow the exposure of the abdominal aorta at the level of the left renal artery. The SMA was carefully cleared of connective tissue immediately distal to where it passed over the caudal vena cava to allow for the perivascular flow probe (1PR,

Transonic Systems, Inc. Ithaca, NY) to be positioned alongside the artery so as not to restrict blood flow.

In animals that were to receive duodenal infusion of a liquid mixed-nutrient mean (Ensure™), a PE-90 catheter was inserted into the proximal duodenum through a small incision in the stomach adjacent to the pylorus and secured with a purse-string suture prior to positioning the perivascular flow probe around the SMA. The Ensure™ was delivered through the catheter by way of a syringe driven by a syringe pump (Razel R99-E, Fisher Scientific) set at an infusion rate of 1 ml/hr.

Laser Doppler flow probe – After placement of the Transonic flow probe and duodenal catheter the retracted viscera were returned to the proper anatomical location. In a subset of the 3 day animals that were simultaneously implanted with the Transonic flow probe (n=8 T3-SCI, n=6 control) and for all 3 week animals that were implanted with the Transonic flow probe (n=5 T3-SCI, n=5 control as enumerated above), a laser Doppler flow probe (BLF22, Transonic Systems, Inc. Ithaca, NY) was positioned in close contact with the mesenteric border of the duodenum immediately distal to the region where the tip of the implanted catheter terminated. Once a stable reading was achieved from the flow probe, the incision was closed around the implanted flow probe and the skin loosely secured with stainless steel wound clips. Animals were allowed to stabilize for 1 hour before data collection was initiated.

Blood Flow Analysis

At the initiation of the stabilization period, the femoral arterial catheter was attached to a pressure transducer (BP-1, World Precision Instruments, Sarasota, FL). Data from the flow meter (T206, Transonic Systems, Inc. Ithaca, NY), blood pressure monitor and laser Doppler flow probe was continuously recorded to computer (Spike 2, Cambridge Electronic Design,

Cambridge, UK). Flow probe signals were filtered at 0.1-10Hz and converted to blood flow in $ml \cdot min^{-1}$ and normalized for body weight. The mean percent change in Doppler output from baseline was calculated for each experimental manipulation. The effect of duodenal infusion was compared to the average blood flow rate of the 10 min preceding the infusion. Peak flow rate was calculated as the highest achieved value during the 1 h following the infusion.

Tissue Harvest

Gastrointestinal tissue - Rats were deeply anesthetized with isoflurane until non-responsive to toe pinch. Quickly, the rats were decapitated and the abdomen was opened via a midline incision. GI tissue (stomach and proximal duodenum) was taken at 1, 3, 7 days, or 3 weeks following T3-SCI or post-control surgery (n=8 per group with one 3 week SCI mortality as noted above). Following GI tissue isolation, a small tissue sample from both the stomach and duodenum, each weighing approximately 200 mg, was removed and placed in aluminum foil and immediately frozen in liquid nitrogen then transferred to a -80°C freezer until used for qRT-PCR. In the same animals, an adjacent section of GI tissue was removed (as above) and placed in room temperature 10% neutral buffered formalin (NBF) for histological processing.

At the conclusion of *in vivo* physiological experiments, deeply anesthetized rats were transcardially perfused with heparinized phosphate-buffered saline (PBS) until fully exsanguinated and followed immediately with PBS containing 4% paraformaldehyde. The spinal cord encompassing the lesion level was removed and refrigerated overnight in PBS containing 20% sucrose and 4% paraformaldehyde.

Histological Processing

Intestine – Formalin fixed tissue from the duodenum 1cm distal to the pylorus were processed in an automated Tissue-Tek VIP processor and paraffin-embedded with a Tissue-Tek

TEC embedding station (Sakura Finetek USA, Torrance, CA). Sections were cut at 6 µm for routine hematoxylin and eosin (H&E) staining.

Intestinal sections were examined by an American College of Veterinary Pathologists diplomate blinded to treatment (author TKC). All images were obtained with an Olympus BX51 microscope and DP71 digital camera using cellSens Standard 1.6 imaging software (Olympus America, Center Valley, PA).

Multiple (3-6) random tissue sections were quantified as described previously (20) and the following measures determined: 1) Villus height and width; 2) Crypt depth and width; and 3) Villus:Crypt height ratio was calculated. In each case, 10 independent measurements for each variable were collected from at least 3 different intestinal sections. Semi-quantitative measurements of inflammation scoring were made on a modified scale (Table 1; adapted from (2) and (4).

Spinal cord lesion center - For histological staining of T3-SCI lesion extent, tissue was sectioned (40µm thick) and alternating sections were mounted on gelatin coated slides. To compare lesion severity with the spinal cords of control animals, spinal cord sections were stained with luxol fast blue (LFB) to visualize myelinated fibers. LFB-stained slides were digitally imaged on a Zeiss Axioscope light microscope and Axiocam CCD camera, imported into Adobe Photoshop and contrast digitally adjusted to allow consistent identification of LFB-stained (i.e., spared) white matter. For individual images, the boundaries of the tissue slice were outlined to determine cross-sectional area. A separate threshold histogram was generated and the pixels corresponding to LFB staining above background were selected. These pixels were quantified and expressed per unit cross-sectional area (38). The lesion epicenter was defined as the section with the least proportion of LFB-stained tissue. The proximity of the T3 lesion center

to the cervical enlargement precluded an appropriate determination of spinal cord cross-sectional area in undamaged tissue rostral to the injury (i.e., damaged tissue extended into the cervical enlargement as described in (60). Therefore, it was necessary that the cross-sectional area of the intact spinal cords at T3 of comparably sized animals be determined for normalization purposes. LFB-stained myelin in injured tissue was then expressed as a percent of the total spinal cord cross-sectional area as would be predicted by the intact tissue.

Based upon previous reports (52, 61, 62) we determined *a priori* that animals sacrificed 3 days following surgery in which LFB staining at the lesion epicenter accounted for ≤ 25% of the region occupied by white matter would be categorized as severe spinal injury; those with ≥ 25% LFB staining were excluded from further analysis (n=6 T3-SCI rats met this critereon). This criterion is based upon the observation that considerable LFB-staining remains within the lesion center in the 1-3 days following injury, though the majority of the LFB-stained tissue likely consists of remaining myelinated axons as well as myelin debris in a loose fibrous matrix as reported previously (62). Historically, our animals with the same 300 kdyne injury that are sacrificed 3 weeks after injury display ≤ 5% of LFB staining above threshold as the lesion center is clear of cellular debris. After 3 weeks any remaining LFB staining is usually confined to a thin band within the ventrolateral white matter in a manner consistent with previous reports characterizing a 200 kdyne injury level (52).

RNA Isolation, Reverse Transcription Reaction and qRT-PCR

Quantitative reverse transcriptase PCR (qRT-PCR) was used to quantify the level of inflammatory mediators present at the assigned time points. Tissue sections from the cranial gastric corpus and proximal duodenum were analyzed for intercellular adhesion molecule-1 (*Icam1*), monocyte chemotactic protein (*Ccl2*), and macrophage inflammatory protein-1α (*Ccl3*),

following T3-SCI and control surgery. Nomenclature is presented according to Rat Genome Nomenclature Committee guidelines (http://www.informatics.jax.org/mgihome/nomen/gene.shtml) along with more common, informal, usage. These particular molecules are commonly reported in the scientific literature and were selected as reliable biomarkers of gastrointestinal pathophysiology (see (19).

Whole GI tissue sections were used for RNA isolation. A small section of GI tissue weighing 50-100 milligrams was cut away from the whole tissue section and used for RNA isolation. RNA was isolated using TRIzol (Invitrogen, Carlsbad, CA) and RNeasy Microkit procedures (Qiagen, Valencia, CA). Briefly, frozen tissue was homogenized in TRIzol using a glass homogenizer and Teflon pestle on ice, chloroform was added to lysate, and the mixture was centrifuged in microcentrifuge tubes to separate RNA. Ethanol was added to the upper aqueous phase, the mixture was applied to an RNeasy spin column and filtered by centrifugation. After several washes, the samples were subjected to an elution step using RNase-free water. Reverse transcription (RT) was conducted using the High Capacity cDNA Reverse Transcription Kit (Applied Biosystems, Foster City, CA). For RT, ~1 μg of RNA from each sample was added to random primers (10×), dNTP (25×), MultiScribe reverse transcriptase (50 U/μl), RT buffer (10×) and RNase Inhibitor (20U/μl) and incubated in a thermal cycler (Techne TC-412, Barloworld Scientific, Burlington, NJ) for 10 min at 25°C, then for 120 min at 37° C. Primers for *Actb* (β-actin) were a QuantiTect Primer Assay (Rn_Actb_1_SG QuantiTect Primer Assay QT00193473, Qiagen, Frederick, MD). Primers for *Icam1*, *Ccl2* (MCP-1) and *Ccl3* (MIP-1α) were designed using Primer Express (Applied Biosystems, Foster City, CA). The forward and reverse primer pairs used for these studies are shown in Table 2.

For real-time PCR, SYBR Green 2× Master Mix (Qiagen), forward and reverse primers (100 μM), and RT product (1μl of a 1:16 dilution) were added to a 384-well plate. The cycling parameters consisted of an initial 2-min incubation at 50°C, followed by 10 min at 95°C, then 15 sec at 95 °C, a 30 sec annealing step at 55°C and a 30 sec extension step at 72°C (55 cycles). A dissociation step (15 sec at 95°C) was added following 55 cycles to determine specificity of primers. In this assay, the dissociation step confirmed the absence of nonspecific amplifications. Quantity of *Icam1*, *Ccl2* (MCP-1), and *Ccl3* (MIP-1α) mRNA was based on a standard curve and normalized to *Actb* (β-actin) mRNA (ABI QuantStudio 12KFlex with available OpenArray block, Applied Biosystems). The suitability of *Actb* as an internal control was assessed through analysis of the raw data between groups and no variability of *Actb* was detected.

Statistical Analysis

Results are expressed as means ± S.E.M. with significance defined as $P < 0.05$. Body weight and MEI measurements from 3 day survival rats did not significantly differ from rats destined to survive 3 weeks. Therefore, these 3 day measures were collapsed for the within groups two-way ANOVA comparison followed by Tukey *post hoc* analysis. Between groups results from *in vivo* blood flow studies were compared by one-way ANOVA and Tukey *post hoc* analysis or paired *t*-test as appropriate. Group results from qRT-PCR were compared by between groups two-way ANOVA and Tukey *post hoc* analysis or paired *t*-test as appropriate. Statistical analysis was performed using SigmaPlot for Windows (SPSS Inc., Chicago, IL).

Results

Assessment of T3-SCI histological severity, reduction of spontaneous feeding and loss of body weight

The severity of experimental T3-SCI was verified based upon the reduction of LFB-stained white matter at the T3 spinal cord segment (Figure 1A). The percent area of white matter at the lesion epicenter of 3 day T3-SCI rats was significantly reduced in comparison to T3-control animals (Figure 1B; $p < 0.05$). At three weeks, when the post-injury progression of the lesion epicenter has relatively stabilized and the lesion boundaries are more clearly defined (22), the percent area of white matter at the lesion epicenter of 3 week T3-SCI rats was significantly reduced in comparison to age-matched T3-control animals (Figure 1B; $p < 0.05$). The data for control animals was pooled in Figure 1B for clarity. These data are comparable to the injury extent reported previously and indicate the severity of our injury model (44, 57, 60, 61).

At 3 days following surgery, the change in body weight between T3-SCI and control animals was -22.5 ± 2.0g vs. 1.2 ± 1.5g, respectively. When normalized as percent of preoperative weight, T3-SCI rats displayed significantly greater weight loss than surgical controls for the comparable time period across the duration of the study (Figure 2A; $p < 0.05$).

Regardless of ease of physical access to chow, spontaneous feeding is suppressed following T3-SCI when gastric motility is compromised. When normalized as the mean energy intake (MEI; defined as kcal/day/100 g body weight) the spontaneous feeding for T3-SCI animals in the present study was significantly lower than controls for every comparable time point until the third week of the study (Figure 2B; $p < 0.05$).

As demonstrated in our previous studies (43, 44, 60), T3-SCI reduced the area of intact white matter, body weight and caloric intake. These data further verify the profound severity, effectiveness and reproducibility of our surgical procedures for T3-SCI and surgical control animals. Based upon these criteria, all animals in these groups were selected for further data analysis.

345

346 *Basal mean arterial blood pressure and mesenteric blood flow are decreased in T3-SCI rats*

347 Prior to the initiation of duodenal nutrient infusion, the baseline systemic mean arterial
348 pressure (MAP) of Inactin-anesthetized T3-SCI rats was significantly lower than the MAP of
349 age-matched surgical control animals (Table 3, Baseline; $p < 0.05$). Following normalization for
350 body weight, basal SMA blood flow in fasted 3 day T3-SCI rats was significantly lower than
351 controls (2.2 ± 0.2 ml/min/100g body weight vs 3.4 ± 0.4 ml/min/100g body weight,
352 respectively; $p < 0.05$). In the age matched cohort of animals tested at 3 weeks after surgery,
353 normalized basal SMA flow was significantly lower in T3-SCI rats compared to controls (1.2 ±
354 0.2 ml/min/100g body weight vs 2.1 ± 0.2 ml/min/100g body weight, respectively; $p < 0.05$).
355 These results confirm that T3-SCI in the rat produces arterial vascular hypotension and
356 hypoperfusion of the splanchnic vascular beds.

357

358 *Postprandial mesenteric arterial reflexes are reduced in T3-SCI rats*

359 Following duodenal infusion of a liquid mixed-nutrient meal (Ensure™, delivered at
360 1ml/hr), T3-SCI rats fail to exhibit the increase in SMA blood flow that is demonstrated by
361 control animals (Figure 3A). During 30 min and 60 min infusion of Ensure™ into the duodenum,
362 the MAP remained significantly different between T3-SCI and control rats (Table 3; $p < 0.05$),
363 however, in both T3-SCI and control rats, duodenal infusion of Ensure™ did not significantly
364 change MAP from pre-infusion baseline values (Table 3; $p > 0.05$).

365 During the 60 minute intra-duodenal infusion of Ensure™, the peak blood flow within
366 the SMA was significantly lower in 3 day T3-SCI rats following the nutrient challenge (Figure
367 3B; $p < 0.05$) compared to controls. This significant difference in peak blood flow persisted in

368 the rats tested 3 weeks after surgery (1.4 ± 0.2ml/min/100g body weight vs. 2.7 ±
369 0.2ml/min/100g body weight; $p < 0.05$). Laser Doppler analysis of the local duodenal perfusion
370 in the region of Ensure™ infusion demonstrated that the percent change in blood flow within the
371 duodenal serosa of surgical control rats was significantly elevated from baseline in comparison
372 to 3 day T3-SCI rats which did not increase during enteral feeding (Figure 3C; $p < 0.05$). At 3
373 weeks after surgery, there was no significant difference in serosal duodenal blood flow between
374 control and T3-SCI rats (127±16% vs. 124±17%, respectively; $p > 0.05$).
375 These results indicate that T3-SCI in the rat diminishes the mesenteric vascular reflexes
376 in response to feeding. Local enterically-mediated changes in duodenal blood flow are also
377 diminished in these same animals during the acute (3 day) phase of injury, but local regulation of
378 duodenal microcirculation returns in longer-term survival periods.
379
380 *T3-SCI provokes gastrointestinal tissue necrosis and shortening of mucosal villi*
381 Upon removal of the GI tract from 3 day T3-SCI animals, it was qualitatively observed
382 that GI mucosal tissue was compromised 3 days following injury compared to controls while
383 mucosal integrity after 3 weeks was unremarkable (Figure 4). For example, sections of the GI
384 tract were described as atrophic, with hemoccult positive contents, and excised tissue was friable
385 (data not shown). Extreme cases also included profound reduction in duodenal integrity and
386 regions of the small intestine revealed necrosis of mucosa and submucosa, neutrophil and
387 macrophage infiltration, and fibroplasia of serosa and submucosa. The duodenum at 3 days
388 following T3-SCI revealed a significant reduction in average mucosal villous height and width
389 (Table 4, $p < 0.05$). The inflammatory score of randomly analyzed tissue segments was

significantly elevated in the duodenum of 3 day T3-SCI rats (Table 4, $p < 0.05$), but not significantly different in 3 week T3-SCI rats (Table 4, $p > 0.05$).

These data demonstrate a continuum of impaired GI tissue health immediately following T3-SCI. Taken together, our anatomical and histological data verify the profound severity produced by our surgical procedures for T3-SCI compared to surgical control animals.

T3-SCI increases upper GI expression of inflammatory markers

To quantify upper GI inflammation, total RNA was isolated to analyze expression of inflammatory markers commonly linked with GI inflammatory processes (19).

In our experimental T3-SCI conditions, gastric *Ccl2* expression was not significantly different between T3-SCI and control (Figure 5A; $p > 0.05$). Gastric expression of the chemokine *Ccl3* demonstrated a significant increase (Figure 5A; $p < 0.05$) at 1 day and 3 days following T3-SCI. However, after 1-week *Ccl3* expression was not significantly different between T3-SCI and control (Figure 5A; $p > 0.05$). The post-SCI expression of *Icam1* demonstrated a significant increase at 1 day and 3 days following T3-SCI that returned to stable levels within 1-week (Figure 5B; $p < 0.05$).

Consistent with our histology findings, duodenal *Ccl2* expression was only significantly different between T3-SCI and control at 3 days after T3-SCI (Figure 6A; $p < 0.05$). Duodenal expression of *Ccl3* demonstrated a significant increase in T3-SCI rats at 1-day after injury (Figure 6B; $p < 0.05$). The significant differences between T3-SCI rats are interpreted to reflect that *Ccl3* returned to low levels beginning at 3 days onwards. The post-SCI expression of *Icam1*, however, demonstrated a significant increase at 1 day and 3 days following T3-SCI (Figure 6C; $p < 0.05$) and returned to low levels by 1-week following T3-SCI. Both control and T3-SCI rats

had a significant increase in *Icam1* levels over the 3 days post-operatively. The principal findings of these data indicate that animals with T3-SCI demonstrate a significant short-term GI inflammatory response immediately following injury.

Discussion

The present experiments demonstrate that systemic cardiovascular derangements at 3 days following a severe T3-SCI include reduced splanchnic vascular competence at rest and following duodenal infusion of a liquid mixed-nutrient meal designed to model clinical enteric supplementation. Specifically, these data indicate that: 1) the anticipated reduction in baseline mean arterial pressure is accompanied by significantly reduced basal blood flow rate through the SMA in rats 3 days after T3-SCI; 2) mean arterial pressure remains at baseline levels in response to enteral administration of a liquid mixed-nutrient meal in both control and T3-SCI rats; 3) T3-SCI rats have a significantly reduced post-prandial mesenteric response following a liquid mixed-nutrient meal; 4) T3-SCI induced a brief, but significant elevation in the gastric expression of inflammatory cytokine transcripts for *Icam1* and *Ccl3* (MIP-1α); and 5) duodenal expression of *Icam1* was most profoundly elevated after T3-SCI. The level of tissue loss at the lesion epicenter, coupled with the observed reduction in feeding and weight loss, is consistent with our previous findings in severe T3-SCI rats that demonstrated gastroparesis and delayed gastric emptying (44, 57, 60). These data lead us to propose that the clinically-recognized vascular reflex deficits in the SCI population may extend to the splanchnic vascular bed that irrigate the GI tissues as demonstrated in our experimental model of high thoracic SCI, though these deficits appear to be only during the early phase of injury. Furthermore, diminished

splanchnic perfusion following T3-SCI may trigger the low grade inflammation observed in GI tissues.

Systemic vascular compromise following T3-SCI

A common consequence of SCI is systemic vascular dysfunction (42). Furthermore, human studies have shown that high-level (cervical) SCIs are accompanied by the most severe hypotension and bradycardia (15-17, 29). The sympathetic preganglionic neurons within the thoracic and lumbar spinal cord normally receive descending inputs, including that from the medullary cardiovascular centers. Interruption of these supraspinal fibers following SCI results in low resting systemic arterial BP, loss of ability to regulate arterial BP, low cardiac output, low venous return, and disturbed reflex control (30, 42). Our acute studies are in agreement with previous observations of a profound reduction in systemic arterial BP after experimental SCI (31, 69). Our observation that arterial BP only partially recovers after 3 weeks is also in agreement with recent temporal studies demonstrating that arterial BP remains chronically suppressed following mid-thoracic spinal transection (69). Beyond the means by which injury was induced, several notable differences exist between our data and the above-mentioned study. The reduction in femoral arterial BP was qualitatively greater in our model than the aortic BP described from the previous report (69). While our studies were in thiobutabarbital-anesthetized rats, rather than telemetrically-implanted awake rats, this particular anesthetic has been reported to have no deleterious effects on cardiovascular function (7). Furthermore, our reduced femoral arterial BP during experimentation was similar to ranges previously reported in chronic SCI rats by Laird and colleagues (31). Therefore, we conclude that our observations are consistent with the post-SCI hypotension reported in the literature.

Visceral hemodynamics following T3-SCI

458 It is estimated that upwards of 70% of blood volume resides within the venous
459 circulation. Vascular stasis coupled with the absence of lower extremity muscle pumps and
460 elevated venous flow resistance leads to venous pooling within extremities. The latter
461 phenomena have been previously reported in experimental models of SCI and may contribute to
462 mesenteric insufficiency (31). Our data demonstrated a reduction in basal blood flow within the
463 SMA. The principal blood supply to the stomach and intestines arises from the gastric branch of
464 the celiac trunk and superior and inferior mesenteric arteries and are collectively referred to as
465 the splanchnic vascular bed. While only one vessel from this triad of splanchnic vessels was
466 monitored, diminished perfusion throughout the splanchnic vascular bed was inferred for all T3-
467 SCI rats.
468 Instances of chronic mesenteric hypoperfusion in atherosclerotic disease or acute
469 mesenteric hypoperfusion following strenuous exercise often report the presentation of
470 abdominal or intestinal angina and hemorrhage (54, 64). With regard to the elderly population,
471 mesenteric stenosis occurs with increasing frequency over 65 years of age (21). Symptomatic
472 presentations were noted to occur during the postprandial phase and underscore the ramifications
473 of widespread insufficiency of splanchnic circulation. Our findings provide initial evidence that
474 the mesentery of SCI subjects may be vulnerable to the pathologies associated with ischemic
475 events.
476 The post-prandial dynamics of blood flow to the splanchnic organs in neurally-in tact
477 animal models has been previously described (11, 58). Postprandial hyperemia in experimental
478 animals subjects consists of a profound increase (ca. 200%) in regional GI blood flow in
479 response to nutrients (35). This redistribution of blood flow is compensated by reflexive
480 increase in cardiac output and a redistribution of flow from other tissues (11). In addition, there

481 is substantial evidence that postprandial hyperemia is locally mediated within the intestinal
482 microvasculature through a complex and not completely understood interplay of local oxygen
483 titers, adenosine levels, prostaglandins, sodium-induced hyperosmolarity and the degree of
484 muscle deformation (39). Ultimately, these changes in microvasculature are under the influence
485 of the hemodynamics of upstream mesenteric arteries. These larger caliber supply arteries and
486 arterioles are under greater influence from extrinsic sympathetic sources (reviewed in (23). One
487 important mechanism in postprandial hyperemia involves the release of GI peptides that have
488 been demonstrated to exert a role in regulating postprandial hemodynamic demand through a
489 centrally mediated reflex (49, 50). Specifically, intestinal cholecystokinin (CCK) and gastric
490 leptin activate subdiaphragmatic vagal afferents that, ultimately, terminate in the nucleus tractus
491 solitarius (NTS). In addition to the role of the NTS toward the modulation of gastric-projecting
492 preganglionic motoneurons in the vagal dorsal motor nucleus (DMN; (46), CCK-sensitive
493 afferents terminate upon a subpopulation of NTS neurons that directly project to select
494 cardiovascular neurons in the rostral ventrolateral medulla (RVLM). Under normal conditions,
495 activation of these RVLM neurons provokes an elevation of systemic sympathetic drive and
496 vasoconstriction within skeletal muscle. Simultaneous input by NTS neurons that project to
497 caudal ventrolateral medulla (CVLM) provokes a reduction in splanchnic sympathetic tone
498 resulting in vasodilation within the mesentery (51). Presympathetic vasomotor projections from
499 both the RVLM and CVLM descend through the spinal cord and are disrupted by T3-SCI. With
500 particular emphasis on the rat, the segmental distribution of identified cardiovascular
501 sympathetic preganglionic neurons begins principally at the second spinal thoracic segment and
502 progresses caudally (18). Evidence from these experiments as well as that gathered from Doppler

blood flow studies of the liver (65) suggests that visceral arterial blood flow is significantly diminished in rats with acute (24-76h) SCI located at, or above mid thoracic (T5) spinal cord.

Inflammation in visceral organs following T3-SCI

While the GI mucosa is a richly perfused vascular bed in health, it is directly juxtaposed with the anaerobic and nonsterile lumen of the gut. As such, intestinal epithelial cells that line the mucosa experience a uniquely steep physiologic oxygen gradient in comparison with other cells of the body. Thus, the intestine is one of the most sensitive tissues to hypoxic insult and even brief periods of GI hypoxia induce the production of inflammatory mediators and dysmotility. Furthermore, there is evidence that hypoxia may be more deleterious to cells than complete anoxia (13). Experimental *in vitro* studies in which mitochondrial or glycolytic metabolism has been disrupted pharmacologically (thereby depleting ATP) have shown that minor reduction in ATP maintained for 12-24 hours is sufficient to induce epithelial monolayer dysfunction (63) . From a clinical standpoint, visceral hypoperfusion in the intensive-care patient leads to hypoxia and initiates an inflammatory cascade with consequent end-organ dysfunction and cervical SCI patients are, indeed, susceptible to multiple organ dysfunction (55). Based upon these observations, the dysregulation of mesenteric blood flow in acutely-injured T3-SCI rats suggests that arterial hypotension consequently diminishes mesenteric blood flow necessary to meet mucosal demands at rest and during digestion. We hypothesized that our observed GI hypoperfusion may be an underlying pathology leading to gastric dysfunction through the generalized mechanism of reduction in energy homeostasis and the initiation of cell damage, destruction, and death due to ischemia (40, 59). Furthermore, it is recognized that ischemia initiates an inflammatory cascade (73). However, caution must be exercised when extrapolating the data from ischemia/reperfusion models and our model of T3-SCI. The acute period of high-level SCI presents severe hypotension requiring vasopressor therapy (reviewed in (66). It is

unclear, however, whether this period of so-called “neurogenic shock” produces a level, and duration, of mesenteric hypoperfusion that is comparable to the approximate 90% reduction of flow seen after SMA occlusion.

The reperfusion of ischemic tissues involves a known, biochemically mediated event involving the increased expression of adhesion molecules and chemokines (41). Beginning with early mast cell degranulation and histamine release (8, 27), the up-regulation of adhesion molecules and chemokines forms the early line of defense in the intestinal mucosa and leads to an inflammatory pathway which promotes neurotoxicity, leukocyte (including lymphocytes, neutrophils, and monocytes), macrophage, and astrocyte recruitment (36), endothelial damage, hypoperfusion, and apoptosis (5, 59, 73). Utilizing our model of acute T3-SCI in rats, we demonstrated the effects of T3-SCI upon *Icam1*, *Ccl2* and *Ccl3* expression within the upper -GI tract which suggests the initiation of a low grade inflammatory cascade following T3-SCI.

Implications of gastrointestinal vascular dysregulation

It is generally recognized that the intestinal tract is acutely sensitive to traumatic events (1). The relationship of properly regulated GI blood flow with patient morbidity or mortality is well recognized in many instances of advanced aging, trauma and critical illness (9, 34, 72). The implications of severely diminished blood flow to the GI tract following SCI are likely to mirror some aspects of these other clinical situations. Other models have shown that ischemic GI tissue reacts by releasing lactate as the mucosal-arterial pCO_2 gradient increases indicating the initiation of anaerobic metabolism in the gut (26) and recruitment of pro-inflammatory cytokines and inflammatory markers. Therefore, if post-SCI hypoperfusion leads to ischemia, tissue damage and necrosis are likely to occur whereby the walls of the GI tract may become permeable, allowing bacteria to proliferate and translocate through the gut wall and into lymph

nodes and blood vessels (6, 32). With inadequate splanchnic perfusion, multiple organ failure and death may ensue (25). The development of episodic hypertension, a phenomenon associated with massive sympathetic discharge that is triggered by noxious visceral or sensory stimuli below the injury level (commonly refered to as autonomic dysreflexia, (24), may also provoke periods of GI hypoxia due to hyperreactivity of the mesenteric bed (47). While the mechanism remains incompletely understood, the impaired GI blood flow we have observed and mesenteric hyperreactivity as is likely to occur during autonomic dysreflexia may contribute to the chronic gastrointestinal dysfunction experienced by individuals with SCI (3, 12, 14, 37, 53, 56, 70).

Conclusion

Our novel data reveal that basal mesenteric blood flow is markedly diminished following a severe spinal cord injury at spinal T3. Furthermore, postprandial splanchnic vascular reflexes are blunted following experimental T3-SCI. We propose that changes in nutrient-vascular relationships may render the post-SCI gut susceptible to episodic ischemic and inflammatory events. Based upon clinical reports, we further propose that these changes in nutrient-vascular relationships may last for weeks after the original SCI and that these co-morbidities may contribute to the GI dysfunction observed in the SCI population.

Acknowledgements

Portions of this data were previously published in abstract form and presented at the National Neurotrauma Society Annual Meetings. Emily Besecker gratefully acknowledges the encouragement and constructive comments of the judges for the National Neurotrauma Society student competition. Dr. Sean Stocker provided guidance for performing and analyzing femoral MAP recording. Margaret McLean assisted with animal care, data entry and analysis in Excel. Preliminary protocols and data supporting this experimental protocol were generated by Emily Qualls-Creekmore at the Pennington Biomedical Research Center, Louisiana State University.

Current address

Emily M. Besecker, PhD, Gettysburg College, Department of Health Sciences, 300 North Washington St., Gettysburg, PA 17325-1400, ebesecke@gettysburg.edu

Grant Support

This work was supported by NIH/NINDS R01NS049177 (G.M. Holmes) and NIH/NINDS F31NS087834 (E.M. Swartz). Training Fellowship support for N. Pironi provided by American Heart Association (12UEFL1008000, S.D. Stocker).

Author Disclosure Statement

No competing financial interests exist for any of the authors.

Author Contributions

584 EMB and GMH designed the study; EMB, NP and GMH and performed *in vivo* studies; GMD
585 performed qRT-PCR and analysis; TKC scored histological specimens. EMB & GMH drafted
586 and revised the manuscript with input from all authors.

587 Reference List

588

589 1. **Bai C, An H, Wang S, Jiang D, Fan W and Nie H**. Treatment and prevention of
590 bacterial translocation and endotoxemia with stimulation of the sacral nerve root in a
591 rabbit model of spinal cord injury. *Spine (Phila Pa 1976)* 36: 363-371, 2011.

592 2. **Berg DJ, Davidson N, Kühn R, Müller W, Menon S, Holland G, Thompson-Snipes**
593 **L, Leach MW and Rennick D**. Enterocolitis and colon cancer in interleukin-10-
594 deficient mice are associated with aberrant cytokine production and CD4(+) TH1-like
595 responses. *J Clin Invest* 98: 1010-1020, 1996.

596 3. **Berlly MH and Wilmot CB**. Acute abdominal emergencies during the first four weeks
597 after spinal cord injury. *Archives of Physical Medicine and Rehabilitation* 65: 687-690,
598 1984.

599 4. **Bleich A, Mahler M, Most C, Leiter EH, Liebler-Tenorio E, Elson CO, Hedrich HJ,**
600 **Schlegelberger B and Sundberg JP**. Refined histopathologic scoring system improves
601 power to detect colitis QTL in mice. *Mamm Genome* 15: 865-871, 2004.

602 5. **Blight AR**. Macrophages and inflammatory damage in spinal cord injury. *J Neurotrauma*
603 9 Suppl 1: S83-S91, 1992.

604 6. **Bohm M, Siwiec RM and Wo JM**. Diagnosis and Management of Small Intestinal
605 Bacterial Overgrowth. *Nutr Clin Pract* 28: 289-299, 2013.

7. **Buelke-Sam J, Holson JF, Bazare JJ and Young JF**. Comparative stability of physiological parameters during sustained anesthesia in rats. *Lab Anim Sci* 28: 157-162, 1978.

8. **Bulmer DCE, Jiang W, Hicks GA, Davis JB, Winchester WJ and Grundy D**. Vagal selective effects of ruthenium red on the jejunal afferent fibre response to ischaemia in the rat. *Neurogastroenterology & Motility* 17: 102-111, 2005.

9. **Casaer MP and Van den Berghe G**. Nutrition in the Acute Phase of Critical Illness. *N Engl J Med* 370: 1227-1236, 2014.

10. **Chou CC**. Splanchnic and overall cardiovascular hemodynamics during eating and digestion. *Fed Proc* 42: 1658-1661, 1983.

11. **Chou CC and Coatney RW**. Nutrient-induced changes in intestinal blood flow in the dog. *Br Vet J* 150: 423-437, 1994.

12. **Cosman BC, Stone JM and Perkash I**. Gastrointestinal complications of chronic spinal cord injury. *J Am Paraplegia Soc* 14: 175-181, 1991.

13. **Dawson TL, Gores GJ, Nieminen AL, Herman B and Lemasters JJ**. Mitochondria as a source of reactive oxygen species during reductive stress in rat hepatocytes. *Am J Physiol* 264: C961-C967, 1993.

14. **Fealey RD, Szurszewski JH, Merritt JL and DiMagno EP**. Effect of traumatic spinal cord transection on human upper gastrointestinal motility and gastric emptying. *Gastroenterology* 87: 69-75, 1984.

15. **Furlan JC and Fehlings MG**. Cardiovascular complications after acute spinal cord injury: pathophysiology, diagnosis, and management. *Neurosurg Focus* 25: E13, 2008.

16. **Furlan JC, Fehlings MG, Shannon P, Norenberg MD and Krassioukov AV**. Descending vasomotor pathways in humans: correlation between axonal preservation and cardiovascular dysfunction after spinal cord injury. *J Neurotrauma* 20: 1351-1363, 2003.

17. **Garstang SV and Miller-Smith SA**. Autonomic nervous system dysfunction after spinal cord injury. *Phys Med Rehabil Clin N Am* 18: 275-vii, 2007.

18. **Gonsalvez DG, Kerman IA, McAllen RM and Anderson CR**. Chemical Coding for Cardiovascular Sympathetic Preganglionic Neurons in Rats. *The Journal of Neuroscience* 30: 11781-11791, 2010.

19. **Granger DN, Holm L and Kvietys P**. The Gastrointestinal Circulation: Physiology and Pathophysiology. In: Comprehensive Physiology, John Wiley & Sons, Inc., 2015.

20. **Gulbinowicz M, Berdel B, Wojcik S, Dziewiatkowski J, Oikarinen S, Mutanen M, Kosma VM, Mykkanen H and Morys J**. Morphometric analysis of the small intestine

in wild type mice C57BL/6L -- a developmental study. *Folia Morphol (Warsz)* 63: 423-430, 2004.

21. **Hansen KJ, Wilson DB, Craven TE, Pearce JD, English WP, Edwards MS, Ayerdi J and Burke GL**. Mesenteric artery disease in the elderly. *J Vasc Surg* 40: 45-52, 2004.

22. **Hill CE, Beattie MS and Bresnahan JC**. Degeneration and sprouting of identified descending supraspinal axons after contusive spinal cord injury in the rat. *Exp Neurol* 171: 153-169, 2001.

23. **Holzer P**. Neural Regulation of Gastrointestinal Blood Flow. In: Physiology of the gastrointestinal tract, edited by Johnson LR, Barrett KE, Ghishan FK, Merchant JL, Said HM and Wood JD. New York: Elsevier Academic Press, 2006.

24. **Hou S and Rabchevsky AG**. Autonomic Consequences of Spinal Cord Injury. In: Comprehensive Physiology, John Wiley & Sons, Inc., 2011.

25. **Jakob SM, Bracht H, Porta F, Balsiger BM, Brander L, Knuesel R, Feng HQ, Kolarova A, Ma Y and Takala J**. Effects of cardiac preload reduction and dobutamine on hepatosplanchnic blood flow regulation in porcine endotoxemia. *Am J Physiol Gastrointest Liver Physiol* 303: G247-G255, 2012.

26. **Jakob SM, Tenhunen JJ, Laitinen S, Heino A, Alhava E and Takala J**. Effects of systemic arterial hypoperfusion on splanchnic hemodynamics and hepatic arterial buffer response in pigs. *Am J Physiol Gastrointest Liver Physiol* 280: G819-G827, 2001.

27. **Jiang W, Kirkup AJ and Grundy D**. Mast cells drive mesenteric afferent signalling during acute intestinal ischaemia. *J Physiol* 589: 3867-3882, 2011.

28. **Kirshblum SC, Groah SL, McKinley WO, Gittler MS and Stiens SA**. Spinal cord injury medicine. 1. Etiology, classification, and acute medical management. *Arch Phys Med Rehabil* 83: S50-S58, 2002.

29. **Krassioukov AV, Karlsson AK, Wecht JM, Wuermser LA, Mathias CJ and Marino RJ**. Assessment of autonomic dysfunction following spinal cord injury: rationale for additions to International Standards for Neurological Assessment. *J Rehabil Res Dev* 44: 103-112, 2007.

30. **Krassioukov A**. Autonomic function following cervical spinal cord injury. *Respir Physiol Neurobiol* 169: 157-164, 2009.

31. **Laird AS, Carrive P and Waite PM**. Cardiovascular and temperature changes in spinal cord injured rats at rest and during autonomic dysreflexia. *J Physiol* 577: 539-548, 2006.

32. **Liu J, An H, Jiang D, Huang W, Zou H, Meng C and Li H**. Study of bacterial translocation from gut after paraplegia caused by spinal cord injury in rats. *Spine* 29: 164-169, 2004.

33. **Lucchini S, Saumet JL, Mei N and Gamier L**. Involvement of the vagus nerve, substance P and cholecystokinin in the regulation of intestinal blood flow. *Journal of the Autonomic Nervous System* 60: 182-192, 1996.

34. **Luciano GL, Brennan MJ and Rothberg MB**. Postprandial Hypotension. *The American Journal of Medicine* 123: 281, 2010.

35. **Matheson PJ, Wilson MA and Garrison RN**. Regulation of Intestinal Blood Flow. *J Surg Res* 93: 182-196, 2000.

36. **Mautes AE, Weinzierl MR, Donovan F and Noble LJ**. Vascular events after spinal cord injury: contribution to secondary pathogenesis. *Phys Ther* 80: 673-687, 2000.

37. **Nino-Murcia M and Friedland GW**. Functional abnormalities of the gastrointestinal tract in patients with spinal cord injuries: Evaluation with imaging procedures. *American Journal of Roentgenology* 158: 279-281, 1991.

38. **Noble LJ and Wrathall JR**. Spinal cord contusion in the rat: morphometric analyses of alterations in the spinal cord. *Exp Neurol* 88: 135-149, 1985.

39. **Nowicki P**. Physiology of the Circulation of the Small Intestine. In: Physiology of the gastrointestinal tract, edited by Johnson LR, Barrett KE, Ghishan FK, Merchant JL, Said HM and Wood JD. New York: Elsevier Academic Press, 2006, p. 1627-1651.

40. **Oruckaptan HH, Ozisik P, Atilla P, Tuncel M, Kilinc K, Geyik PO, Basaran N, Yuksel E and Ozcan OE**. Systemic administration of interleukin-10 attenuates early ischemic response following spinal cord ischemia reperfusion injury in rats. *J Surg Res* 155: 345-356, 2009.

41. **Oz OE, Korkmaz A, Kardess O and Omeroglu S**. Aortic cross-clamping-induced spinal cord oxidative stress in rabbits: the role of a novel antioxidant adrenomedullin. *J Surg Res* 147: 143-147, 2008.

42. **Popa C, Popa F, Grigorean VT, Onose G, Sandu AM, Popescu M, Burnei G, Strambu V and Sinescu C**. Vascular dysfunctions following spinal cord injury. *J Med Life* 3: 275-285, 2010.

43. **Primeaux SD, Tong M and Holmes GM**. Effects of chronic spinal cord injury on body weight and body composition in rats fed a standard chow diet. *Am J Physiol Regul Integr Comp Physiol* 293: R1102-R1109, 2007.

44. **Qualls-Creekmore E, Tong M and Holmes GM**. Time-course of recovery of gastric emptying and motility in rats with experimental spinal cord injury. *Neurogastroenterol Motil* 22: 62-e28, 2010.

45. **Qualls-Creekmore E, Tong M and Holmes GM**. Gastric emptying of enterally administered liquid meal in conscious rats and during sustained anaesthesia. *Neurogastroenterol Motil* 22: 181-185, 2010.

46. **Rogers RC, Hermann GE and Travagli RA**. Brainstem Control of the Gastric Function. In: Physiology of the gastrointestinal tract, edited by Johnson LR, Barrett KE, Ghishan FK, Merchant JL, Said HM and Wood JD. New York: Elsevier Academic Press, 2006, p. 851-875.

47. **Rummery NM, Tripovic D, McLachlan EM and Brock JA**. Sympathetic vasoconstriction is potentiated in arteries caudal but not rostral to a spinal cord transection in rats. *Journal of Neurotrauma* 27: 2077-2089, 2010.

48. **Sánchez-Fernández C, González MC, Beart PM, Mercer LD, Ruiz-Gayo M and Fernández-Alfonso MS**. A novel role for cholecystokinin: regulation of mesenteric vascular resistance. *Regulatory Peptides* 121: 145-153, 2004.

49. **Sartor DM, Shulkes A and Verberne AJM**. An enteric signal regulates putative gastrointestinal presympathetic vasomotor neurons in rats. *Am J Physiol Regul Integr Comp Physiol* 290: R625-R633, 2006.

50. **Sartor DM and Verberne AJM**. Cholecystokinin selectively affects presympathetic vasomotor neurons and sympathetic vasomotor outflow. *Am J Physiol Regul Integr Comp Physiol* 282: R1174-R1184, 2002.

51. **Sartor DM and Verberne AJM**. Abdominal vagal signalling: A novel role for cholecystokinin in circulatory control? *Brain Research Reviews* 59: 140-154, 2008.

52. **Scheff SW, Rabchevsky AG, Fugaccia I, Main JA and Lumpp J-EJ**. Experimental modeling of spinal cord injury: characterization of a force-defined injury device. *J Neurotrauma* 20: 179-193, 2003.

53. **Segal JL, Milne N and Brunnemann SR**. Gastric emptying is impaired in patients with spinal cord injury. *American Journal of Gastroenterology* 90: 466-470, 1995.

54. **Silva JA and White CJ**. Ischemic Bowel Syndromes. *Primary Care: Clinics in Office Practice* 40: 153-167, 2013.

55. **Stein D, Menaker J, McQuillan K, Handley C, Aarabi B and Scalea T**. Risk Factors for Organ Dysfunction and Failure in Patients with Acute Traumatic Cervical Spinal Cord Injury. *Neurocritical Care* 13: 29-39, 2010.

56. **Stinneford JG, Keshavarzian A, Nemchausky BA, Doria MI and Durkin M**. Esophagitis and esophageal motor abnormalities in patients with chronic spinal cord injuries. *Paraplegia* 31: 384-392, 1993.

57. **Swartz EM and Holmes GM**. Gastric vagal motoneuron function is maintained following experimental spinal cord injury. *Neurogastroenterol Motil* 27: 2-7, 2014.

58. **Takagi T, Naruse S and Shionoya S**. Postprandial celiac and superior mesenteric blood flows in conscious dogs. *Am J Physiol* 255: G522-G528, 1988.

59. **Temiz C, Solmaz I, Tehli O, Kaya S, Onguru O, Arslan E and Izci Y**. The effects of splenectomy on lipid peroxidation and neuronal loss in experimental spinal cord ischemia/reperfusion injury. *Turk Neurosurg* 23: 67-74, 2013.

60. **Tong M and Holmes GM**. Gastric dysreflexia after acute experimental spinal cord injury in rats. *Neurogastroenterol Motil* 21: 197-206, 2009.

61. **Tong M, Qualls-Creekmore E, Browning KN, Travagli RA and Holmes GM**. Experimental spinal cord injury in rats diminishes vagally-mediated gastric responses to cholecystokinin-8s. *Neurogastroenterol Motil* 23: e69-e79, 2011.

62. **Totoiu MO and Keirstead HS**. Spinal cord injury is accompanied by chronic progressive demyelination. *The Journal of Comparative Neurology* 486: 373-383, 2005.

63. **Unno N, Menconi MJ, Salzman AL, Smith M, Hagen S, Ge Y, Ezzell RM and Fink MP**. Hyperpermeability and ATP depletion induced by chronic hypoxia or glycolytic inhibition in Caco-2BBe monolayers. *Am J Physiol* 270: G1010-G1021, 1996.

64. **van Wijck K, Lenaerts K, Grootjans J, Wijnands KAP, Poeze M, van Loon LJC, Dejong CHC and Buurman WA**. Physiology and pathophysiology of splanchnic hypoperfusion and intestinal injury during exercise: strategies for evaluation and

762 prevention. *American Journal of Physiology - Gastrointestinal and Liver Physiology* 303:
763 G155-G168, 2012.

764 65. **Vertiz-Hernandez A, Castaneda-Hernandez G, Martinez-Cruz A, Cruz-Antonio L,**
765 **Grijalva I and Guizar-Sahagun G**. L-arginine reverses alterations in drug disposition
766 induced by spinal cord injury by increasing hepatic blood flow. *J Neurotrauma* 24: 1855-
767 1862, 2007.

768 66. **Weaver LC, Fleming JC, Mathias CJ and Krassioukov AV**. Chapter 13 - Disordered
769 cardiovascular control after spinal cord injury. In: Handbook of Clinical Neurology.
770 Spinal Cord Injury, edited by Joost Verhaagen and John. Elsevier, 2012, p. 213-233.

771 67. **Wehner S, Behrendt FF, Lyutenski BN, Lysson M, Bauer AJ, Hirner A and Kalff**
772 **JC**. Inhibition of macrophage function prevents intestinal inflammation and postoperative
773 ileus in rodents. *Gut* 56: 176-185, 2007.

774 68. **West CR, Alyahya A, Laher I and Krassioukov A**. Peripheral vascular function in
775 spinal cord injury: a systematic review. *Spinal Cord* 51: 10-19, 2013.

776 69. **West CR, Popok D, Crawford MA and Krassioukov AV**. Characterizing the Temporal
777 Development of Cardiovascular Dysfunction in Response to Spinal Cord Injury. *Journal*
778 *of Neurotrauma* 32: 922-930, 2015.

70. **Williams RE, Bauman WA, Spungen AM, Vinnakota RR, Farid RZ, Galea M and Korsten MA**. SmartPill technology provides safe and effective assessment of gastrointestinal function in persons with spinal cord injury. *Spinal Cord* 50: 81-84, 2011.

71. **Wolf C and Meiners TH**. Dysphagia in patients with acute cervical spinal cord injury. *Spinal Cord* 41: 347-353, 2003.

72. **Yang S, Wu X, Yu W and Li J**. Early Enteral Nutrition in Critically Ill Patients With Hemodynamic Instability: An Evidence-Based Review and Practical Advice. *Nutr Clin Pract* 29: 90-96, 2014.

73. **Zhu P, Li JX, Fujino M, Zhuang J and Li XK**. Development and treatments of inflammatory cells and cytokines in spinal cord ischemia-reperfusion injury. *Mediators Inflamm* 2013: 701970, 2013.

Figure 1.

A. Luxol-stained white matter from T3 spinal cords of control, 3 day postoperative (*middle*) and 3 weeks post operative (*right*) rats (scale bar = 1mm).

B. Graphic summary of the percent sparing of white matter at the lesion epicenter of control, 3 day or 3 week rats following a 300-kdyne contusion SCI (* $p<0.05$ vs. age-matched controls; † $p<0.05$ vs. 3 day T3-SCI).

Figure 2. Post-operative body weight and food intake are significantly lower in T3-SCI animals.

Compared to age-matched control animals, the post-operative body weight (expressed as percent of pre-operative weight) is significantly lower following T3-SCI for the duration of the experiment (A). The mean energy intake is significantly reduced following T3-SCI for the first two weeks when compared to their age-matched cohort (B). For all measures * $p<0.05$ vs. age-matched control.

Figure 3. Post-prandial hyperemia is significantly lower in T3-SCI animals.

Representative traces (A) illustrating the normal post-prandial hyperemia from a 3 day control rat (top trace) while post-prandial SMA blood flow from 3 day T3-SCI rats (second trace) did not demonstrate a response to duodenal perfusion of a mixed-nutrient meal (Ensure™; infusion of rate was 1ml/hr). This disruption of postprandial response continued through 3 weeks following T3-SCI. Arrows depict the initiation of Ensure™ administration for each representative subject. (B) The peak volume of SMA blood flow reached during the intra-duodenal infusion period was also significantly reduced in 3 day and 3 week T3-SCI rats. (C) Local tissue perfusion was measured by Laser Doppler Flow of the duodenal serosa. Compared to controls , the percent change in Doppler signal vs. baseline flow was significantly lower only in 3 day T3-SCI rats.

Values expressed as mean ± SEM; * $P<0.05$ vs. control.

Figure 4. Representative images of H&E-stained duodenal sections after T3-SCI or control surgery.

T3-SCI provokes altered mucosal architecture as evidenced by blunting of intestinal villi at 3 days following T3-SCI when compared to surgical control animals. After 3 weeks, the height and width of intestinal villi was similar for both T3-SCI and control animals. (X100, scale bar 200 μm).

Figure 5. Expression levels of gastric inflammatory markers mRNA after T3-SCI.

A) Gastric Ccl2 (MCP-1) mRNA expression was not significantly altered in T3-SCI rats. B) Gastric *Ccl3* (MIP-1α) mRNA expression demonstrated a significant (between-groups) elevation in T3-SCI rats at 1 day and 3 days compared to control animals matched for the same post-operative time point (denoted by lowercase a). C) Gastric *Icam1* mRNA expression was significantly elevated in T3-SCI rats at 1 day and 3 days compared to control animals matched for the same post-operative time point. Levels of *Ccl3* and *Icam1* returned to baseline by 1 week post-injury. $P<0.05$, based on ANOVA, followed by Tukey *post hoc* test. (values expressed as mean ± SEM).

Figure 6. Expression levels of duodenal inflammatory marker mRNA after T3-SCI .

A) Duodenal *Ccl2* (MCP-1) mRNA expression demonstrated a significant elevation in T3-SCI rats only at the 3 day post-operative time point compared to control animals. B) The expression of duodenal *Ccl3* (MIP-1α) mRNA demonstrated a significant elevation in T3-SCI rats only at 1 day post-injury compared to control animals matched for the same post-operative time point. Expression levels for T3-SCI returned to baseline by 3 days post-op. C) duodenal *Icam1* mRNA expression demonstrated a significant elevation in T3-SCI rats at 1 day post-injury and continuing through 3 days post-injury compared to control animals at the same post-operative time point. The peak response for T3-SCI rats occurred in 3 day survival rats. Levels of *Ccl2, Ccl3* and *Icam1* returned to baseline within 1 week post-injury.. $P<0.05$, based on ANOVA, followed by Tukey *post hoc* test. (values expressed as mean ± SEM).

848

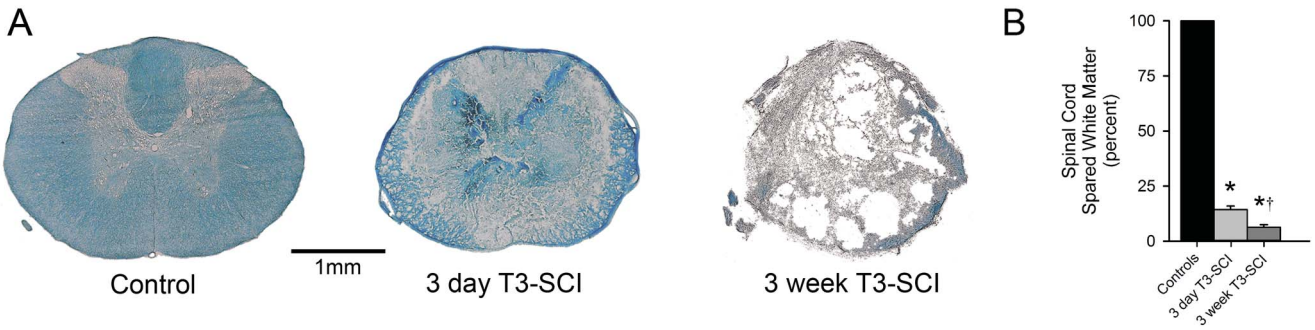
A
Control
1mm
3 day T3-SCI
3 week T3-SCI
B
Spinal Cord
Spared White Matter
(percent)
100
75
50
25
0
*
*†
Controls
3 day T3-SCI
3 week T3-SCI

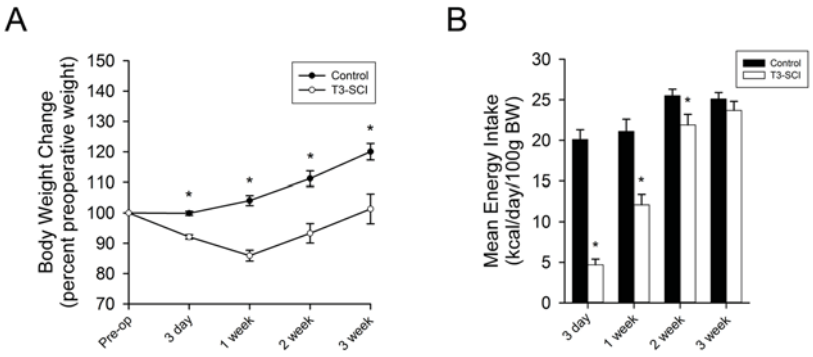
A
Body Weight Change
(percent preoperative weight)
150
140
130
120
110
100
90
80
70
Control
T3-SCI
*
*
*
*
Pre-op
3 day
1 week
2 week
3 week
B
Mean Energy Intake
(kcal/day/100g BW)
30
25
20
15
10
5
0
Control
T3-SCI
*
*
*
3 day
1 week
2 week
3 week

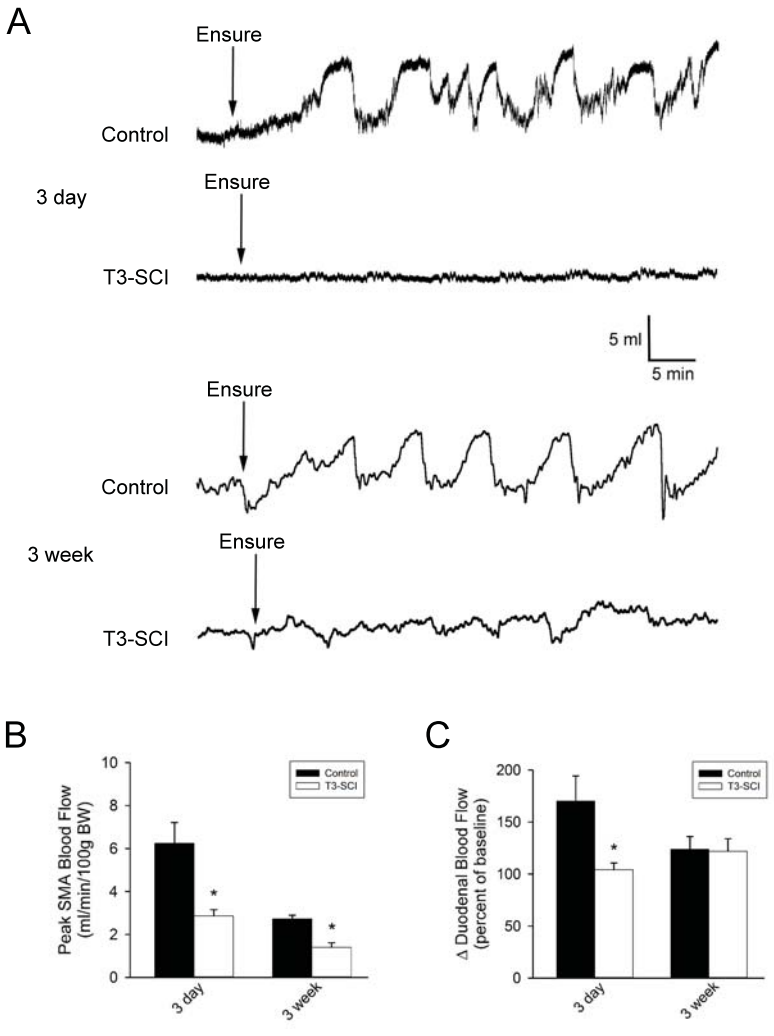
A
Ensure
Control
3 day
Ensure
T3-SCI
5 ml
5 min
Ensure
Control
3 week
Ensure
T3-SCI
B
Peak SMA Blood Flow
(ml/min/100g BW)
10
8
6
4
2
0
Control
T3-SCI
*
*
3 day
3 week
C
Δ Duodenal Blood Flow
(percent of baseline)
200
150
100
50
0
Control
T3-SCI
*
3 day
3 week

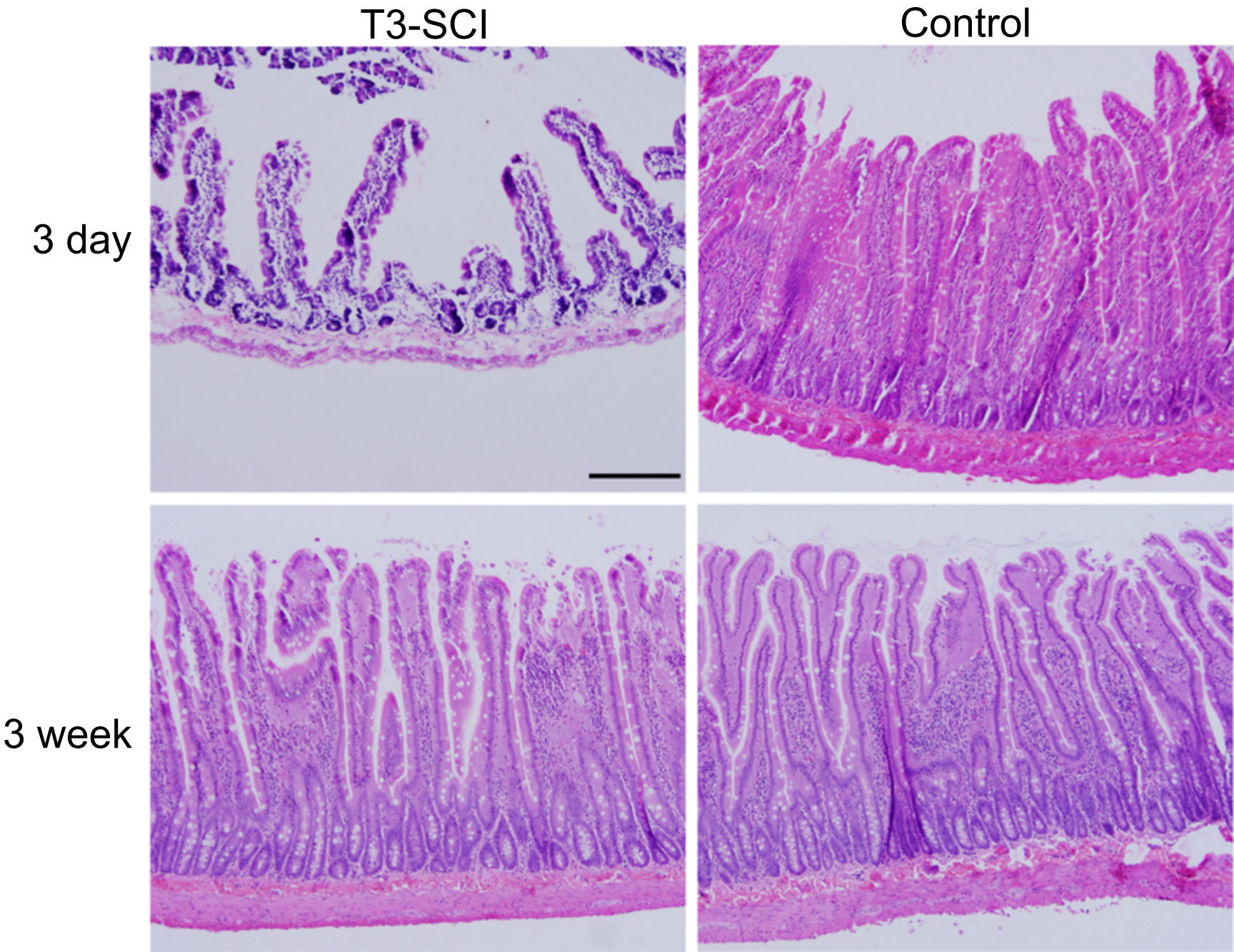
T3-SCI
Control
3 day
3 week

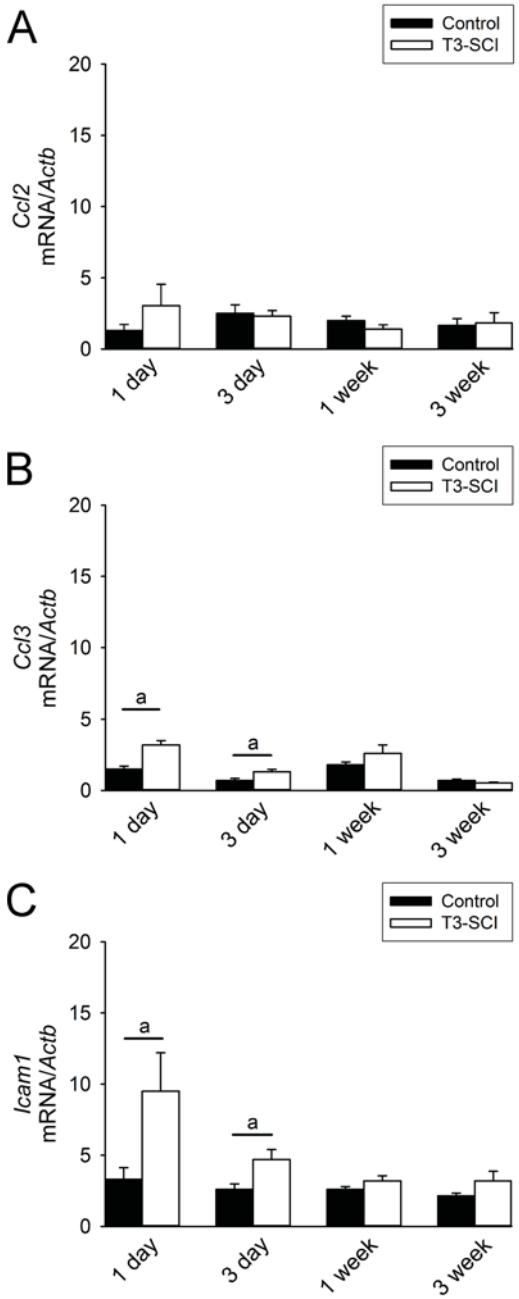
A
Control
T3-SCI
Ccl2 mRNA/Actb
20
15
10
5
0
1 day
3 day
1 week
3 week
B
Control
T3-SCI
Ccl3 mRNA/Actb
a
a
20
15
10
5
0
1 day
3 day
1 week
3 week
C
Control
T3-SCI
Icam1 mRNA/Actb
a
a
20
15
10
5
0
1 day
3 day
1 week
3 week

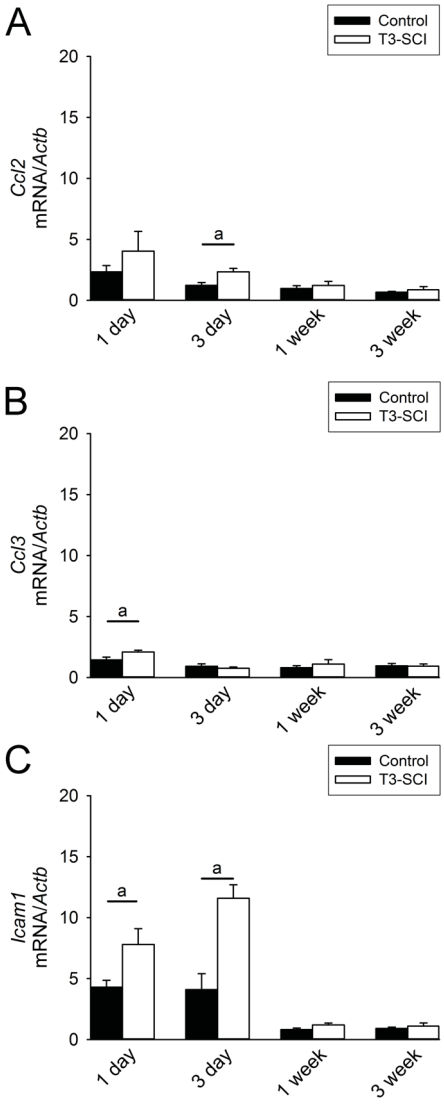
A
Control
T3-SCI
Ccl2
mRNA/Actb
20
15
10
5
0
a
1 day
3 day
1 week
3 week
B
Control
T3-SCI
Ccl3
mRNA/Actb
20
15
10
5
0
a
1 day
3 day
1 week
3 week
C
Control
T3-SCI
Icam1
mRNA/Actb
20
15
10
5
0
a
a
1 day
3 day
1 week
3 week

Table 1

Semi-quantitative measurements of inflammation scoring for gastrointestinal tissue	
Grade	Description
Grade 0:	No change from normal tissue
Grade 1:	One or a few multifocal mononuclear cell infiltrates in the lamina propria
Grade 2:	Lesions involve more of the intestine than grade 1 lesions, and/or are more frequent. Typical changes include several multifocal, mild inflammatory cell infiltrates in the lamina propria composed primarily of mononuclear cells with a few neutrophils. Inflammation rarely involves the submucosa
Grade 3:	Lesions involve a large area of the mucosa or are more frequent than grade 2 lesions. Inflammation is moderate and involves the submucosa but is not transmural. Inflammatory cells are a mixture of mononuclear cells as well as neutrophils, and crypt abscesses are sometimes observed. Small epithelial erosions are occasionally present.
Grade 4:	Lesions involve most of the intestinal section and are more severe than grade 3 lesions. Inflammation is severe, including mononuclear cells and neutrophils, and can be transmural. Crypt abscesses and ulcers are present.

Table 2

Forward and reverse primer sequences for quantitative real time PCR (qRT-PCR)

Gene	Forward Primer	Reverse Primer
Ccl2 (MCP-1)	5'-TCTCTGTCACGCTTCTGGGCCT-3'	5'-TAGCAGCAGGTGAGTGGGGCA-3'
Ccl3 (MIP-1α)	5'-TGACACCCCGACTGCCTGCT-3'	5'-TGACACCCGGCTGGGACCAA-3'
Icam1	5'-TGCCAGCCCGGAGGATCACA-3'	5'-CGGGAGCTAAAGGCACGGCA-3'

Table 3

Mean arterial pressure (mmHg) is not altered by Ensure™ infusion in 3 day T3-SCI, 3 day surgical controls, 3 week T3-SCI and 3 week controls.

	Baseline	30 min infusion	60 min infusion
3 day Control	112.9 ± 4.3	109.2 ± 2.4	105.2 ± 5.0
3 day T3-SCI	74.8 ± 4.9*	69.9 ± 5.7*	65.9 ± 7.0*
3 week Control	127.5 ± 6.1	122.0 ± 4.5	112.8 ± 3.2
3 week T3-SCI	90.2 ± 3.4**	90.8 ± 4.2**	88.6 ± 3.2**

Values presented as mean ± SEM. *P<0.05 vs 3 day control. **P<0.05 vs 3 week control

Table 4

T3-SCI provokes an inflammatory response and blunting of mucosal villi in duodenal tissue at 3 days after injury (*p<0.05 vs. control).

		Experimental Groups	
		Control	T3-SCI
3 day	Average inflammatory score	0.4 ± 0.2	0.9 ± 0.1 *
	Average villus height (µm)	435 ± 24	341 ± 11 *
	Average villus width (µm)	122 ± 4	102 ± 2 *
	Average crypt depth (µm)	149 ± 6	147 ± 10
	Average crypt width (µm)	52 ± 2	52 ± 2
	Villus:crypt ratio	3 ± 0.1	2 ± 0.2
	Villus height:width ratio	4 ± 0.2	3 ± 0.2
		Control	T3-SCI
3 week	Average inflammatory score	1.75 ± 0.9	1.75 ± 0.1
	Average villus height (µm)	513 ± 12	491 ± 23
	Average villus width (µm)	121 ± 4	113 ± 4
	Average crypt depth (µm)	178 ± 8	201 ± 8
	Average crypt width (µm)	48 ± 1	44 ± 1
	Villus:crypt ratio	3 ± 0.1	2 ± 0.1
	Villus height:width ratio	4 ± 0.2	4 ± 0.1